Table 1. Lack of anaphylactic shock in rats infused with EV

Infusion	1st	2nd	3rd	4th
EV (n = 3)	Alive with symptomless	Alive with symptomless	Alive with symptomless	Alive with symptomless
Saline (n = 3)	Alive with symptomless	Alive with symptomless	Alive with symptomless	Alive with symptomless
OVA (n = 3)	Alive with symptomless	Dead within 3 min with respiratory distress		

DISCUSSION

In the previous study, Rabinovici et al. reported that LEH induced a hematological response in rats, such as an increase of WBC and a decrease of PLT within 5–25 min after the infusion, but these changes returned to basal levels 2 h after the infusion [32]. However, we did not observe the effects of HbV infusion in such a short period, and the numbers of RBC, WBC and PLT were unchanged in the three groups during the observation period of one week Figure 1. Although the numbers of WBC did not differ among the three groups, a significant change of the ratios of lymphocytes and granulocytes was observed at 6 h after the infusion (Figure 2). The degree of these changes was greater in the HbV group than in the EV group. Similarly, Rudolph et al. reported that the polymorphonuclear leukocyte counts were increased and lymphocyte counts were decreased 2 h after the LEH infusion, except that their change was correlated with the increase of WBC [33]. We also observed that the ratios of monocytes dropped 6 h after the infusion, even in the saline group, and gradually returned to the initial level. However, the reasons for these phenomena are unexplainable at present.

The ratio of $CD4^+$ T cells and $CD8^+$ T cells is an important indicator of the immune system in subjects. In immune compromised patients, such as AIDS, an inversion of the $CD4^+/CD8^+$ ratio is a typical event due to an increase in the absolute number of $CD8^+$ cells [34]. In this study, the $CD4^+/CD8^+$ ratio was not inverted and was constant in each group during the observation period (Figure 3). Although a significant difference between the HbV and EV groups and control group was observed on day 1, the implication of this significance for an immune response may be less important because the $CD4^+/CD8^+$ ratio was not inverted and lower in HbV and EV groups than in the control group, even at the pre-infusion time, due to unknown reasons.

As mentioned in the previous study [19], the influence of liposomes on the complement is a considerable subject to assess the safety of liposomal therapeutics. The complement plays a role in subjects not only as a defense system, but also as causal agents for adverse reactions when it is activated in excess. The considerable characters of liposomes and other things are as follows: negatively charged surface [35–37], cholesterol contents [35,38], and the existence of natural anti-phospholipid antibodies in subjects [20]. Complement activation induces a pseudoallergic reaction in the pig model [21,22], and hypotension, flushing, respiratory distress, decrease of mean arterial pressure and chest pain in humans [39,40]. We previously reported that HbV does not activate the complement *in vitro* using human serum [19]. In this study, we examined the effect of HbV on the complement using rats *in vivo* and *in vitro*. The *in vitro* study showed that the complement titer in the HbV group was equivalent to that in the control group, indicating that HbV did not consume the complement of rat serum (Fig. 5). The *in vivo* study, however, showed that the complement titer dropped by 9% on day 3 and 14% on day 7 after the HbV infusion, and then returned to the initial level (Fig. 4). No allergic reaction was observed in these rats. In contrast, another study reported that complement consumption *in vivo* occurred immediately (i.e. within 10–120 min) in rats after the infusion of LEH, which has the ability to activate complement *in vitro* [41]. Therefore, the gradual drop of complement titer in rats in this study is unlikely to be due to the complement consumption, but some impairment in the metabolic or synthetic function of complement may be underlying the mechanisms of this phenomenon.

To further examine the decline of the complement titer by HbV, a repeated-infusion study was performed. Additional HbV was infused at two-day intervals because the decline of complement titer was remarkable on day 3 after the HbV infusion. Very interestingly, only the first infusion reduced the complement titer and, thereafter, the recovery of the complement titer occurred gradually despite additional HbV being infused (Fig. 6). Namely, the additional HbV infusion did not induce the further decline of the complement titer. These results also indicate that the transient drop of complement titer is not due to the complement consumption that resulted from the direct interaction between HbV and the complement components. As mentioned above, the gradual drop of the complement titer is probably due to yet unknown mechanisms other than consumption. However, such unknown mechanisms were not enhanced by the additional HbV infusion. Therefore, the precise mechanisms of the decrease of the complement titer induced by HbV infusion remain to be clarified with great interest.

To investigate whether HbV would induce anaphylactic or pseudoallergic reactions, rats were sensitized several times with EV at appropriate

intervals. Because HbV would be administered intravenously in clinical settings, the first administration of EV was performed intravenously. On the other hand, OVA as a positive control was subcutaneously administered with the adjuvant to obtain a complete immunization. Although three administrations were carried out after the first EV infusion, no clinical modulation was observed while the OVA-sensitized rats resulted in death after the second administration. These results suggest that HbV may induce neither anaphylactic nor allergic reaction in subjects, possibly also including humans.

Finally, HbV induced a transient change in the leukocyte population, but not in the RBC, WBC or PLT counts. In addition, the $CD4^+/CD8^+$ ratio was maintained at a reasonable level without the inversion of the ratio. Although the complement titer transiently dropped on day 3 after the HbV infusion, the decline was not considered to be the complement consumption and the degree of the decline is unlikely to affect host defense. In addition, repeated HbV infusion also revealed that the influence of HbV on complement was transient and an additional four HbV infusions did not induce the further decline of the complement titer. Furthermore, no anaphylactic reaction was observed in multiple EV infusions. In conclusion, from a clinical point of view, HbV induced no serious side-effects regarding the subjects in this study, and is a promising material to be safely administrable as an artificial oxygen carrier.

REFERENCES

1. Bunn, H.F., Esham, W.T., Bull, R.W. (1969). The renal handling of hemoglobin. I. Glomerular filtration. *J. Exp. Med.* **129**: 909–923.
2. Martin, W., Villani, G.M., Jothianandan, D., Furchgott, R.F. (1985). Selective blockade of endothelium-dependent and glyceryl trinitrate-induced relaxation by hemoglobin and by methylene blue in the rabbit aorta. *J. Pharmacol. Exp. Ther.* **232**: 708–716.
3. Hess, J.R., MacDonald, V.W., Brinkley, W.W. (1993). Systemic and pulmonary hypertension after resuscitation with cell-free hemoglobin. *J. Appl. Physiol.* **74**: 1769–1778.
4. Chang T.M. (1964). Semipermeable microcapsules. *Science.* **146**: 524–525.
5. Chang T.M. (1971). Stabilisation of enzymes by microencapsulation with a concentrated protein solution or by microencapsulation followed by cross-linking with glutaraldehyde. *Biochem. Biophys. Res. Commun.* **44**:1531–1536.
6. Chatterjee, R., Welty, E.V., Walder, R.Y., Pruitt, S.L., Rogers, P.H., Arnone, A., Walder, J.A. (1986). Isolation and characterization of a new hemoglobin derivative cross-linked between the a chains (lysine 99a1-lysine 99a2). *J. Biol. Chem.* **261**: 9929–9937.
7. DeVenuto, F., Zegna, A. (1983). Preparation and evaluation of pyridoxalated-polymerized human hemoglobin. *J. Surg. Res.* **34**: 205–212.

8. Ajisaka, K., Iwashita, Y. (1980). Modification of human hemoglobin with polyethylene glycol: a new candidate for blood substitute. *Biochem. Biophys. Res. Commun.* **97**: 1076–1081.
9. Lieberthal, W., Fuhro, R., Andry, C., Valeri, C.R. (2000). Effects of hemoglobin-based oxygen-carrying solutions in anesthetized rats with accute ischemic renal failure. *J. Lab. Clin. Med.* **135**: 73–81.
10. Raat, N.J., Liu, J.F., Doyle, M.P., Burhop, K.E., Klein, J., Ince, C. (2005). Effects of recombinant-hemoglobin solutions rHb2.0 and rHb1.1 on blood pressure, intestinal blood flow, and gut oxygenation in a rat model of hemorrhagic shock. *J. Lab. Clin. Med.* **145**: 9–11.
11. Djordjevich, L., Miller, I.F. (1980). Synthetic erythrocytes from lipid encapsulated hemoglobin. *Exp. Hematol.* **8**: 584–592.
12. Gaber, B.P., Farmer, M.C. (1984). Encapsulation of hemoglobin in phospholipid vesicles: Preparation and properties of a red cell surrogate. *Prog Clin Biol Res.* **165**: 179–190.
13. Hunt, C.A., Burnette, R.R., MacGregor, R.D., Strubbe, A.E., Lau, D.T., Taylor, N., Kiwada, H. (1985). Synthesis and evaluation of a prototypal artificial red cell. *Science* **230**: 1165–1168.
14. Rudolph, A.S., Klipper, R.W., Goins, B., Phillips, W.T. (1991). In vivo biodistribution of a radiolabeled blood substitute: 99mTc-labeled liposome-encapsulated hemoglobin in an anesthetized rabbit. *Proc Natl Acad Sci USA.* **88**: 10976–10980.
15. Phillips, W.T., Klipper, R.W., Awasthi, V.D., Rudolph, A.S., Cliff, R., Kwasiborski, V., Goins, B.A. (1999). Polyethylene glycol-modified liposome-encapsulated hemoglobin: A long circulating red cell substitute. *J. Pharmacol Exp. Ther.* **288**: 665–670.
16. Wakamoto, S., Fujihara, M., Abe, H., Sakai, H., Takeoka, S., Tsuchida, E., Ikeda, H., Ikebuchi, K. (2001). Effects of poly(ethyleneglycol)-modified hemoglobin vesicles on agonist-induced platelet aggregation and RANTES release in vitro. *Artif. Cells Blood Substit. Immobil. Biotechnol.* **29**: 191–201.
17. Wakamoto, S., Fujihara, M., Abe, H., Yamaguchi, M., Takeoka, S., Tsuchida, E., Azuma, H., Ikeda, H. (2005). Effects of hemoglobin vesicles on resting and agonist-stimulated human platelets in vitro. *Artif. Cells Blood Substit. Biotechnol.* **33**: 101–111.
18. Ito, T., Fujihara, M., Abe, H., Yamaguchi, M., Wakamoto, S., Takeoka, S., Sakai, H., Tsuchida, E., Ikeda, H., Ikebuchi, K. (2001). Effects of poly(ethyleneglycol)-modified hemoglobin vesicles on *N*-formyl-methionyl-leucyl-phenylalanine-induced responses of polymorphonuclear neutrophils in vitro. *Artif. Cells Blood Substit. Immobil. Biotechnol.* **29**: 427–437.
19. Abe, H., Fujihara, M., Ikebuchi, K., Takeoka, S., Tsuchida, E., Harashima, H., Azuma, H., Ikeda, H. (2006). Interaction of hemoglobin vesicles, a cellular-type artificial oxygen carrier, with human plasma: Effects on coagulation, kallikrein-kinin, and complement systems. *Artif. Cells Blood Substit. Biotechnol.* **34**: 1–10.
20. Szebeni, J., Wassef, N.M., Rudolph, A.S., Alving, C.R. (1996). Complement activation in human serum by liposome-encapsulated hemoglobin: The role of natural anti-phospholipid antibodies. *Biochim. Biophys. Acta* **1285**: 127–130.

21. Szebeni, J., Baranyi, L., Savay, S., Bodo, M., Morse, D.S., Basta, M., Stahl, G.L., Bunger, R., Alving, C.R. (2000). Liposome-induced pulmonary hypertension: Properties and mechanism of a complement-mediated pseudoallergic reaction. *Am. J. Physiol. Heart Circ. Physiol.* **279**: H1319–H1328.
22. Laverman, P., Boerman, O.C., Oyen, W.J.G., Corstens, F.H.M., Storm, G. (2001). *In vivo* applications of PEG liposomes: Unexpected observations. *Crit. Rev. Ther. Drug Carrier Syst.* **18**: 551–566.
23. Sakai, H., Takeoka, S., Wettstein, R., Tsai, A.G., Intaglietta, M., Tsuchida, E. (2002). Systemic and microvascular responses to hemorrhagic shock and resuscitation with Hb vesicles. *Am. J. Physiol. Heart Circ. Physiol.* **283**: H1191–1199.
24. Sakai, H., Masada, Y., Horinouchi, H., Yamamoto, M., Ikeda, E., Takeoka, S., Kobayashi, K., Tsuchida, E. (2004). Hemoglobin-vesicles suspended in recombinant human serum albumin for resuscitation from hemorrhagic shock in anesthetized rats. *Crit. Care Med.* **32**: 539–545.
25. Yoshizu, A., Izumi, Y., Park, S., Sakai, H., Takeoka, S., Horinouchi, H., Ikeda, E., Tsuchida, E., Kobayashi, K. (2004). Hemorrhagic shock resuscitation with an artificial oxygen carrier, hemoglobin vesicle maintains intestinal perfusion and suppresses the increase in plasma tumor necrosis factor-alpha. *ASAIO J.* **50**: 458–463.
26. Sakai, H., Horinouchi, H., Masada, Y., Takeoka, S., Ikeda, E., Takaori, M., Kobayashi, K., Tsuchida, E. (2004). Metabolism of hemoglobin-vesicles (artificial oxygen carriers) and their influence on organ functions in a rat model. *Biomaterials.* **25**: 4317–4325.
27. Sakai, H., Takeoka, S., Park, S.I., Kose, T., Nishide, H., Izumi, Y., Yoshizu, A., Kobayashi, K., Tsuchida, E. (1997). Surface modification of hemoglobin vesicles with poly(ethylene glycol) and effects on aggregation, viscosity, and blood flow during 90% exchange transfusion in anesthetized rats. *Bioconjug. Chem.* **8**: 23–30.
28. Sou, K., Naito, Y., Endo, T., Takeoka, S., Tsuchida, E. (2003). Effective encapsulation of proteins into size-controlled phospholipid vesicles using freeze-thawing and extrusion. *Biotechnol. Prog.* **19**: 1547–1552.
29. Abe, H., Ikebuchi, K., Hirayama, J., Fujihara, M., Takeoka, S., Sakai, H., Tsuchida, E., Ikeda, H. (2001). Virus inactivation in hemoglobin solution by heat treatment. *Artif. Cells Blood Substit. Immobil. Biotechnol.* **29**: 381–388.
30. Singh, P., Daniels, M., Winsett, D.W., Richards, J., Doerfler, D., Hatch, G., Adler, K.B., Gilmour, M.I. (2003). Phenotypic comparison of allergic airway responses to house dust mite in three rat strains. *Am. J. Physiol. Lung Cell Mol. Physiol.* **284**: L588–L598.
31. Kurebayashi, Y., Honda, Y. (1991). Protection by 16,16-dimethyl prostaglandin E2 and dibutyryl cyclic AMP against complement-mediated hepatic necrosis in rats. *Hepatology* **14**: 545–550.
32. Rabinovici, R., Rudolph, A.S., Feuerstein, G. (1989). Characterization of hemodynamic, hematologic, and biochemical responses to administration of liposome-encapsulated hemoglobin in the conscious, freely moving rat. *Circulatory Shock* **29**: 115–132.

33. Rudolph, A.S., Cliff, R.O., Spargo, B.J., Spielberg, H. (1994). Transient changes in the mononuclear phagocyte system following administration of the blood substitute liposome-encapsulated haemoglobin. *Biomaterials* **15**: 796–804.
34. Cooper, D.A., Tindall, B., Wilson, E.J., Imrie, A.A., Penny, R. (1988). Characterization of T lymphocyte responses during primary infection with human immunodeficiency virus. *J. Infect. Dis.* **157**: 889–896.
35. Cunningham, C.M., Kingzette, M., Richards, R.L., Alving, C.R., Lint, T.F., Gewurz, H. (1979). Activation of human complement by liposomes: A model for membrane activation of the alternative pathway. *J. Immunol.* **122**: 1237–1242.
36. Chonn, A., Cullis, P.R., Devine, D.V. (1991). The role of surface charge in the activation of the classical and alternative pathways of complement by liposomes. *J. Immunol.* **146**: 4234–4241.
37. Devine, D.V., Wong, K., Serrano, K., Chonn, A., Cullis, P.R. (1994). Liposome-complement interactions in rat serum: Implications for liposome survival studies. *Biochim. Biophys. Acta* **1191**: 43–51.
38. Alving, C.R., Richards, R.L., Guirguis, A.A. (1977). Cholesterol-dependent human complement activation resulting in damage to liposomal model membranes. *J. Immunol.* **118**: 342–347.
39. Laing, R.B., Milne, L.J., Leen, C.L., Malcolm, G.P., Steers, A.J. (1994). Anaphylactic reactions to liposomal amphotericin. *Lancet* **344**: 682.
40. Ringden, O., Andstrom, E., Remberger, M., Svahn, B.M., Tollemar, J. (1994). Allergic reactions and other rare side-effects of liposomal amphotericin. *Lancet* **344**: 1156–1157.
41. Szebeni, J., Wassef, N.M., Spielberg, H., Rudolph, A.S., Alving, C.R. (1994). Complement activation in rats by liposomes and liposome-encapsulated hemoglobin: Evidence for anti-lipid antibodies and alternative pathway activation. *Biochem. Biophys. Res. Commun.* **205**: 255–263.

Journal of Biomedical Materials Research Part A

Early View (Articles online in advance of print)
Published Online: 6 Feb 2008

Influence of hemoglobin vesicles, cellular-type artificial oxygen carriers, on human umbilical cord blood hematopoietic progenitor cells *in vitro*

Miki Yamaguchi [1], Mitsuhiro Fujihara [1]*, Shinobu Wakamoto [1], Hiromi Sakai [2], Shinji Takeoka [3], Eishun Tsuchida [2], Hiroshi Azuma [1], Hisami Ikeda [1]

[1]Japanese Red Cross, Hokkaido Red Cross Blood Center, Yamanote 2-2, Nishi-Ku, Sapporo 063-0002, Japan

[2]Research Institute for Science and Engineering, Waseda University, 3-4-1 Okubo, Shujuku, Tokyo 169-8555, Japan

[3]Consolidated Research Institute for Advanced Science and Medical Care, Waseda University, 3-4-1 Okubo, Sinjuku, Tokyo 169-8555, Japan

email: Mitsuhiro Fujihara (fujihara@hokkaido.bc.jrc.or.jp)

*Correspondence to Mitsuhiro Fujihara, Japanese Red Cross, Hokkaido Red Cross Blood Center, Yamanote 2-2, Nishi-Ku, Sapporo 063-0002, Japan

Funded by:

- Health and Labor Sciences Research Grants (Research on Regulatory Science of Pharmaceuticals and Medical Devices)
- Ministry of Health, Labor and Welfare, Japan
- Oxygenix Inc., Tokyo, Japan

KEYWORDS

liposome-encapsulated hemoglobin ◆hemoglobin-vesicles ◆hematopoietic progenitor cells ◆colony assay ◆biocompatibility

ABSTRACT

Hemoglobin vesicles (HbVs), liposomal oxygen carriers containing human hemoglobin, are candidates for development as clinically useful blood substitutes. Although HbVs are shown to distribute transiently into the bone marrow in animal models, the influence of HbVs on human hematopoietic stem/progenitor cells has not yet been studied. Therefore, we investigated the influence of HbVs at a concentration of up to 3 vol/vol % on the clonogenic activity (in semisolid culture) and proliferative activity (in liquid culture) of human hematopoietic progenitor cells derived from umbilical cord blood (CB) *in vitro*. Continuous exposure of CB mononuclear cells to HbVs tended to decrease the number and size of mature-committed colonies and most notably reduced the number of colonies of high-proliferative potential colony-forming cells (HPP-CFC). In contrast, exposure to HbVs for 20 h or 3 days, which is more relevant to the clinical setting, had no effect on the number of mature-committed colonies and only modestly decreased the number of HPP-CFC. Continuous exposure (10 days) to HbVs significantly suppressed the cellular proliferation and differentiation of both the erythroid and myeloid lineages in liquid culture. Again, short exposure (20 h or 3 days) did not affect these parameters. Thus, our results show that HbVs, under conditions relevant to the clinical setting, have no adverse effect on human CB hematopoietic progenitor activity *in vitro*. © 2008 Wiley Periodicals, Inc. J Biomed Mater Res 2008

Received: 25 April 2007; Revised: 21 August 2007; Accepted: 16 October 2007

DIGITAL OBJECT IDENTIFIER (DOI)

10.1002/jbm.a.31857 About DOI

ARTICLE TEXT

INTRODUCTION

Hemoglobin vesicles (HbVs) or liposome-encapsulated Hbs comprise human hemoglobin encapsulated within a phospholipid bilayer membrane and have been developed as an artificial oxygen carrier.[1-3] Several studies have demonstrated that the HbVs transport oxygen as efficiently as red blood cells,[4-7] making them a promising candidate for clinical trials.

HbVs are injected intravenously, therefore, the biocompatibility of HbVs with blood components is of primary importance to ensure the safety of these materials for clinical use. We have evaluated this biocompatibility by investigating the influence of HbVs on human blood cells as well as plasma *in vitro* and shown that HbVs are highly biocompatible with human blood.[8-10]

It has been clearly demonstrated that intravenously injected liposome products for drug delivery are eventually captured by the reticuloendothelial system (RES), such as Kupffer cells in the liver and macrophages in the spleen and bone marrow.[11] A study in which technetium-99m-labeled HbVs were infused into animals demonstrated that the HbVs were mainly distributed in the liver, spleen and bone marrow,[12] and another histopathological study clarified that the HbVs are promptly metabolized in the RES.[13] Because the clinical utilization of an artificial oxygen carrier as a transfusion alternative would result in the substitution of a large volume of blood, it is important to elucidate the influence of HbVs on subsequent hematopoiesis. There has been concern over whether the HbVs distributed into bone marrow might adversely affect hematopoiesis, because the bone marrow is the major site of hematopoiesis. From this point of view, rats that received an acute 40% exchange-transfusion with HbVs showed complete recovery of the hematocrit within 7 days due to the elevated erythropoietic activity.[14] Furthermore, the number of red blood cells, leukocytes, and platelets remained unchanged for 1 week after the infusion of HbVs at 20% of the whole blood volume.[15] The findings in these animal models strongly suggest the absence of inhibitory activity of HbVs against hematopoiesis. However, the influence of HbVs on the human hematopoietic stem/progenitor cells has not yet been studied.

In vitro models of hematopoiesis, such as colony-forming assays, have been widely used to investigate the proliferation and differentiation of both of pluripotent hematopoietic stem cells and different progenitor cells of blood cell lineages [e.g., burst-forming units of erythrocyte (BFU-E) and colony-forming units of granulocytes/macrophages (CFU-GM)]. These techniques appear to be useful for investigating the pathogenic mechanisms of drug-induced blood disorders and also

for screening the safety of compounds in preclinical testing.[16]

In this study, therefore, we sought to evaluate the influence of HbVs on the clonogenic activity of human umbilical cord blood (CB) hematopoetic cells, which are rich in hematopoietic stem/progenitor cells. In addition, we investigated the effect of HbVs on the proliferation and differentiation of both the erythroid and myeloid lineages of CB hematopoietic cells in liquid culture.

MATERIAL AND METHODS

HbVs

HbVs were prepared under sterile conditions, as described previously.[17][18] The Hb was purified from outdated donated blood provided by the Japanese Red Cross Society (Tokyo, Japan). The encapsulated Hb solution (38 g/dL) contained 14.7 mmol/L pyridoxal 5′-phosphate (PLP) as an allosteric effector at a molar ratio of [PLP]/[Hb] of 2.5. The lipid bilayer was composed of 1,2-dipalmitoyl-*sn*-glycero-3-phosphatidylcholine, cholesterol, 1,5-*O*-dihexadecyl-*N*-succinyl-L-glutamate (Nippon Fine Chemical, Osaka, Japan), and 1,2-distearoyl-*sn*-glycero-3-phosphatidylethanolamine-*N*-[poly(ethylene glycol) (5,000)] (NOF, Tokyo, Japan) at a molar ratio of 5:5:1:0.033. In some experiments, empty liposomes, which have the same constituents as HbVs, except for the absence of Hb, were used. The concentration of lipopolysaccharide, measured by a modified Limulus test, was less than 0.4 EU/mL.[19] The physicochemical parameters were P_{50}, 27 Torr; 262 ± 77-nm particle diameter; and MetHb content <3%. The concentration of Hb in the HbVs dispersion was adjusted to 10 g/dL. The concentration of HbVs in this study was set at about 3 vol/vol %, based on the following rationale. Intravenously injected HbVs are eventually captured by phagocytes in the RES, including the spleen, liver, and bone marrow. The half-life of HbVs in the circulation in humans has been estimated to be 66 h by the study of circulation kinetics using rats and rabbits,[12] and the percent infused dose of HbVs of bone marrow in humans was estimated to be 6.4% at 48 h after 25% top loading of HbVs, in studies of the organ distribution of HbVs in rats and rabbits.[12] Based on this estimation, the distribution of HbVs in the human bone marrow at 48 h after infusion at 25 vol/vol % (1225 mL of HbVs) of the blood volume (4.9 L, 70 mL/kg, body weight) in a 70-kg individual may be expected to be 78.4 mL (6.4 vol/vol % of the infused dose of HbVs). The volume of the bone marrow space has been estimated as 2.6-4 L in an average-sized human (70 kg).[20] From these values, the amount of HbVs in the human bone marrow can be calculated to be about 2-3 vol/vol %.

Preparation of human CB

Use of human umbilical CB for the experiments was approved by the Committee of Hokkaido CB Bank. CB was obtained during normal full-term deliveries. CB $CD34^+$ cells were prepared as described previously.[21] In brief, after sedimentation of red blood cells by incubating the CB samples with the same volume of 6% (w/v) hydroxyethyl starch dissolved in Ringer's solution (Veen-D, Nikken Chemical, Tokyo, Japan) at room temperature for 30 min, the low-density (<1.077 g/mL) mononuclear cells were collected with Ficoll-Paque (Pharmacia Biotech, Uppsala, Sweden). For some experiments, the cells were further enriched with $CD34^+$ cells using a MACS CD34 Progenitor Isolation Kit (Milenyi Biotech, Bergish-Gladbach, Germany) according to the manufacturer's instructions. In all experiments, the purity of the $CD34^+$ cells was >85%.

Clonal cell culture

The methylcellulose clonal culture was performed in 35-mm suspension culture dishes (Nippon

Becton Dickinson [BD], Tokyo, Japan). The population of $CD34^+$ cells among the mononuclear cells was determined by flow cytometry, and the CB-derived mononuclear cells were seeded at 300 $CD34^+$ cells/dish. A complete methylcellulose medium for human clonal culture assays (Methocult GFH4434V; StemCell Technologies, Vancouver BC, Canada) was used. The presence of up to 3% HbVs did not interfere with the microscopic detection of the colonies formed.

After 14 days incubation at 37°C in a humidified atmosphere containing 5% CO_2, the BFU-E, CFU-GM, CFU-Mix, and colony-forming units in culture (CFU-C) were scored under an inverted microscope. Densely packed colonies that reached >1 mm in size were scored as high proliferative potential colony-forming cells (HPP-CFC) after 28 days incubation. In some experiments, the CB-derived mononuclear cells were suspended to obtain 1500 $CD34^+$ cells/mL in Iscove's modified Dulbecco's medium (IMDM, Gibco BRL, Rockville, MD) containing 30% FCS (Equitech Bio, Igram, TX), 1% bovine serum albumin (BSA; Sigma Chemical, St Louis, MO), 10 ng/mL human interleukin-3 (IL-3), 10 ng/mL human stem cell factor (SCF, provided by Kirin Brewery, Tokyo, Japan), 10 ng/mL granulocyte colony-stimulating factor (G-CSF, a gift from Chugai Pharmaceutical, Tokyo, Japan), and 50 U/mL granulocyte-macrophage colony-stimulating factor (GM-CSF; Schering Research, Bloomfield, NJ). Then, different concentrations of HbVs were added to the cell suspension. The cells were incubated either for 20 h or for 3 days. Subsequently, they were recovered, washed to remove the HbVs, and resuspended in 5 mL of MethoCult GF. One milliliter of the resultant cell suspension (by adjusting $CD34^+$ cells to 300 cells/dish) was seeded into a 35-mm dish for the clonal assay.

Liquid culture

$CD34^+$ cells enriched from CB-derived mononuclear cells were suspended in 4 mL of the following culture media and seeded in 12.5-cm^2 flasks (Nippon BD, Tokyo, Japan). The culture medium for the erythroid lineage was IMDM-containing 30% FBS, 1% BSA, 10 ng/mL human IL-3, 10 ng/mL human SCF, and 2 U/mL human erythropoietin (provided by Chugai Pharmaceutical). The culture medium for the myeloid lineage was IMDM-containing 30% FBS, 1% BSA, 50 μM β-mercaptoethanol, 10 ng/mL human IL-3, 10 ng/mL human SCF, 10 ng/mL G-CSF, and 50 U/mL GM-CSF. These combinations of cytokines have been shown to promote proliferation and differentiation of $CD34^+$ cells toward mature erythroid and myeloid lineage cells, respectively.[22][23] Various concentrations of HbVs were added to the medium containing the cells. After 10 days incubation at 37°C in a humidified atmosphere containing 5% CO_2, the total cell counts were determined. $CD235a^+$ (glycophorin A) cells for the erythroid lineage and $CD15^+$ cells for the myeloid lineage, respectively, were analyzed by flow cytometry. For determining the effects of short-term exposure, the cells were incubated with HbVs for either 20 h or 3 days, washed to remove the HbVs, and then incubated for a total of 10 days.

Flow-cytometric analysis

Aliquots of cells were stained with monoclonal antibodies in PBS/0.1% BSA at 4°C for 30 min. The analysis was performed using a BD LSR flow cytometer (BD Biosciences Immunocytometry System, San Diego, CA). The following monoclonal antibodies were used: FITC-conjugated CD34 (Nippon Becton Dickinson [BD]) antibody, PE-conjugated CD235a and CD33 (DAKO) antibodies, FITC-conjugated CD15 (DAKO) antibody, and APC-conjugated CD45 (BD) antibody. FITC- and PE-conjugated mouse IgG1 antibodies (BD), APC-conjugated mouse IgG1 (BD), and FITC-conjugated IgM (DAKO) antibodies were used as isotype-matched controls. In the flow-cytometric analysis, dead cells were gated out first by propidium iodide staining and then with a forward versus side scatter window. For each analysis set, at least 10,000 events were collected.

Histological staining

Cultured cells (1×10^3 - 1×10^4/100 μL) were centrifuged onto slides with Cytospin (Shandon, Pittsburgh, PA) and stained with May-Grünwald-Giemsa (Merck, Darmstadt, Germany). Microscopic images were captured with an MP5Mc/OL digital camera (Olympus) and processed using Win Roof software, version 5.5.

Statistical analysis

Results are expressed as mean ± standard deviation (SD). A two-way paired ANOVA followed by *post hoc* Bonferroni's test was used for comparisons of multiple HbV-treated groups with the control (HbV; 0%) group. For analysis of the difference between two exposure times, unpaired two-tailed Student's *t* test was used. Values of $p < 0.05$ were considered significant.

RESULTS AND DISCUSSION

Clonogenic potential of CB hematopoietic cells

We first examined the effect of continuous exposure to HbVs (0.09%-3%) on the formation of BFU-E, CFU-GM, CFU-Mix, CFC, and HPP-CFC in the clonogenic assay. HbVs at 3% inhibited the formation of CFU-GM and tended to decrease the formation of CFC-C. Most notably, HbVs significantly inhibited the formation of HPP-CFC in a concentration-dependent manner (Fig. 1A). Although no change in the number of colonies of BFU-E was noted, the size of the colonies of BFU-E and CFU-GM tended to be smaller in the presence than in the absence of HbVs (Fig. 2). On the other hand, the empty liposomes (phospholipid vesicles devoid of Hb) had no inhibitory effect on the formation of mature-committed colonies or HPP-CFC (Fig. 1B).

Figure 1. A: Effects of HbVs on the clonogenic activity of CB-derived hematopoietic cells. B: Effects of empty liposomes on the clonogenic activity of CB-derived hematopoietic cells. CB-derived mononuclear cells were seeded at 300 $CD34^+$ cells per dish in complete methylcellulose medium for human clonal-culture assays. Various concentrations of HbVs or empty liposomes (vol/vol %) were added to the medium containing the cells. BFU-E, CFU-GM, CFU-Mix, and CFU-C were scored after 14 days incubation. HPP-CFC was scored after 28 days incubation. Data represent the mean ± SD of three experiments performed on three separate CB donors in (A) and (B), respectively. A two-way paired ANOVA followed by Bonferroni's test was used for comparisons of multiple HbVs-treated groups with the control (HbVs; 0%) group. *$p < 0.05$, **$p < 0.01$ versus HbVs (0%).
[Normal View 84K | Magnified View 262K]

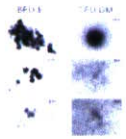

Figure 2. Effects of HbVs on the size of the colonies of BFU-E and CFU-GM formed in clonal cultures of CB-derived cells. Representative colonies of BFU-E and CFU-GM in the absence and presence of HbVs are shown. Scales represent 50 μm.
[Normal View 28K | Magnified View 103K]

As continuous exposure to HbVs had a marked inhibitory effect on the formation of HPP-CFC, we examined the effect of short-term exposure of CB hematopoietic cells to HbVs. Toward this end, the CB hematopoietic cells were exposed to HbVs for 20 h or for 3 days, washed to remove the HbVs, and then subjected to a clonogenic assay. Exposure to HbVs for 20 h had no inhibitory effect on the formation of either HPP-CFC or other mature-committed colonies (Fig. 3). Exposure to 3% HbVs for 3 days modestly inhibited the formation of HPP-CFC, however, a greater number

of HPP-CFC was formed when compared with that observed under continuous exposure to HbVs. No effect was observed on the formation of other mature-committed colonies (Fig. 3). From the clinical point of view, continuous exposure of hematopoietic stem/progenitor cells to HbVs in the marrow for 14 days or 28 days is unlikely. Rather, 1-3 days exposure is more relevant to the clinical setting as described below. In this sense, short-term exposure of hematopoietic progenitor cells to HbVs even at 3% had no adverse effect on the clonogenic activity of hematopoietic progenitor cells.

Figure 3. Effects of short-term exposure to HbVs on the clonogenic activity of CB-derived hematopoietic cells. CB-derived mononuclear cells were suspended in IMDM containing FCS, BSA, IL-3, SCF, G-CSF, and GM-CSF; then, different concentrations of HbVs were added to the cell suspension. The cells were incubated for 20 h (open column) or for 3 days (closed column). Subsequently, they were recovered, washed to remove the HbVs, and subjected to clonal assay. Data were expressed as the mean ± SD of the percentage of control. Three experiments were performed on three separate CB donors. **$p < 0.01$; 20 h versus 3-day exposure; unpaired Student's *t* test.
[Normal View 15K | Magnified View 33K]

Proliferation and differentiation of erythroid or myeloid lineage cells from CB hematopoietic progenitor cells in liquid culture

Because the numbers of HPP-CFC and CFU-GM were significantly reduced, and the size of the colonies of BFU-E and CFU-GM tended to be smaller in the presence than in the absence of HbVs, we next examined the effect of HbVs (0.75%, 1.5%, or 3%) on the proliferation of erythroid or myeloid lineage cells in a liquid culture of CB $CD34^+$ cells. As shown in Figure 4, the presence of HbVs throughout the culture period significantly inhibited the proliferation of $CD235a^+$ cells (erythroid lineage) and $CD15^+$ (myeloid lineage) cells in a dose-dependent manner. These results suggested that continuous exposure to HbVs had an inhibitory effect on the proliferation of hematopoietic progenitor cells. Thus, the reduced number of HPP-CFC and reduced colony size of BFU-E and CFU-GM in the clonogenic assay were surmised to be associated with reduced proliferation of the erythroid and myeloid lineage cells in the presence of HbVs throughout the culture period.

Figure 4. Effects of HbVs on the proliferation of erythroid lineage (left panel) or myeloid lineage cells (right panel) from CB-derived hematopoietic progenitor cells in liquid culture. Various concentrations of HbVs were added to medium containing the CB-derived $CD34^+$ cells. After 10 days' incubation, $CD235a^+$ cells for the erythroid lineage and $CD15^+$ cells for the myeloid lineage, respectively, were analyzed by flow cytometry. Data represent the mean ± SD of six experiments performed on six separate CB donors. A two-way paired ANOVA followed by Bonferroni's test was used for comparisons of multiple HbVs-treated groups with the control (HbVs; 0%) group. **$p < 0.01$ versus HbVs (0%).
[Normal View 7K | Magnified View 15K]

We further analyzed the subset of $CD235a^+$ cells and $CD15^+$ cells. The $CD235a^+CD45^-$ cells and $CD15^+CD33^-$ cells represented some of the more differentiated cells in the erythroid and myeloid lineage, respectively. Continuous exposure to HbVs significantly reduced the percentage of

$CD233^+CD45^-$ cells in the total cell population (Fig. 5A). Microscopic examination of a smear of cells cultured for 10 days revealed that while orthochromatic erythroblasts and erythrocytes (differentiated lineage) were present in the absence of HbVs, basophilic erythroblasts (less differentiated lineage) were more abundant in the presence of 3% HbVs (Fig. 5B).

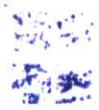

Figure 5. Effects of HbVs on the differentiation of erythroid cells from CB-derived hematopoietic progenitor cells in liquid culture. CB-derived $CD34^+$ cells were cultured in the medium for induction of erythroid lineage without or with HbVs (0.75%, 1.5%, or 3.0%). A: The percentage of $CD235a^+$ $CD45^-$ cells in the total cell population was analyzed by flow cytometry. Data represent the mean ± SD of experiments performed on CB obtained from six separate donors. A two-way paired ANOVA followed by Bonferroni's test was used for comparisons of multiple HbVs-treated groups with the control (HbVs 0%) group. $*p < 0.05$, $**p < 0.01$ versus HbVs (0%). Representative results of flow cytometric analysis are shown at the bottom. B: Morphology of the cells generated in the liquid culture for erythroid lineage. Arrow head; basophilic erythroblasts, white arrow; orthochromatic erythroblasts, and black arrow; erythrocyte. Note that the differentiated erythroid cells are much fewer in number in the presence of HbVs when compared with that in the control (HbVs 0%). [Color figure can be viewed in the online issue, which is available at www.interscience.wiley.com.]
[Normal View 58K | Magnified View 221K]

Similarly, continuous exposure to HbVs significantly decreased the percentage of $CD15^+CD33^-$ cells in the total cell population (Fig. 6A). Examination of a smear of the cells showed that while metamyelocytes (differentiated lineage) could be recognized in the absence of HbVs, myelocytes (less differentiated lineage) were more abundant in the presence of 3% HbVs (Fig. 6B). These results suggest that continuous exposure to HbVs also inhibited the differentiation of both erythroid and myeloid lineage cells.

Figure 6. Effects of HbVs on the differentiation of myeloid cells from CB-derived hematopoietic progenitor cells in liquid culture. CB-derived $CD34^+$ cells were cultured in the medium for the induction of myeloid lineage without or with HbVs (0.75%, 1.5% or 3.0%). A: The percentage of $CD15^+$ $CD33^-$ cells in the total cell population was analyzed by flow cytometry. Data represent the mean ± SD of experiments performed on six separate CB donors. A two-way paired ANOVA followed by Bonferroni's test was used for the comparisons of multiple HbVs-treated groups with the control (HbVs 0%) group. $*p < 0.05$, $**p < 0.01$ versus HbVs (0%). Representative results of flow cytometric analysis are shown at the bottom. B: Morphology of the cells generated in the liquid culture for erythroid lineage. Arrow head, macrophage; white arrow, myelocyte; and black arrow, metamyelocyte. Note that the differentiated myeloid cells are much fewer in number in the presence of HbVs when compared with that in the control (HbVs 0%). Scales represent 10 μm. [Color figure can be viewed in the online issue, which is available at www.interscience.wiley.com.]
[Normal View 43K | Magnified View 170K]

Next, the effects of the short exposure to HbVs, which is more relevant to the clinical setting, of

$CD34^+$ cells on the proliferative activity of both erythroid and myeloid lineage cells were examined. Exposure to HbVs even at 3% for 20 h or for 3 days did not affect the proliferative activity of either the $CD235a^+$ cells or the $CD15^+$ cells (Fig. 7). Furthermore, the percentages of $CD235a^+CD45^-$ cells and $CD15^+CD33^-$ cells in the total cell population were not affected by exposure to HbVs, either for 20 h or for 3 days (data not shown). Thus, HbVs exerted no inhibitory effects on the proliferation and differentiation of either erythroid or myeloid lineage cells following short durations of exposure.

Figure 7. Effects of HbVs on the proliferation of erythroid lineage (left panels) or myeloid lineage (right panels) cells from CB-derived hematopoietic progenitor cells in liquid culture. CB-derived $CD34^+$ cells were exposed to HbVs (0%, 0.75%, 1.5%, or 3%) for 20 h, 3 days, or 10 days. After culture for a total of 10 days, $CD235a^+$ cells for the erythroid lineage and $CD15^+$ cells for the myeloid lineage, respectively, were analyzed by flow cytometry. The number of $CD235a^+$ cells or $CD15^+$ cells at each concentration of HbVs is expressed as a percentage of the number in the control (HbVs 0%). Data represent the mean ± SD of three experiments performed on three separate CB donors. A two-way paired ANOVA followed by Bonferroni's test was used for comparisons of multiple HbVs-treated groups with the control (HbVs 0%) group. $*p < 0.05$, $**p < 0.01$ versus HbVs (0%).
[Normal View 30K | Magnified View 78K]

Several hypotheses have been suggested to explain the inhibitory effects of continuous exposure to HbVs on hematopoietic progenitor activity including direct contact of the progenitor cells with HbVs, conversion of Hb in HbVs to met-Hb during culture, interaction of progenitor cells with several components from HbVs, which might degrade over time. The observation that the empty liposomes did not have any inhibitory effect on the clonogenic activity suggested that the progenitor activity was not inhibited by direct contact of the progenitor cells with the HbVs surface, but by the presence of Hb in the HbVs. In this case, higher dissolved oxygen concentrations in the culture medium were theoretically expected in the presence of HbVs than in the absence of HbVs, which may be involved in the inhibition of progenitor activity following to the prolonged exposure to HbVs. Furthermore, conversion of Hb to met-Hb within HbVs[24] cannot be excluded as the reason for the inhibition of progenitor activity caused by HbVs. In addition, there is a possibility that HbVs might degrade during long-term incubation, leading to the release of Hb. We determined the Hb level during the continuous presence of HbVs in liquid culture up to 10 days. At maximum, 6.7% of the Hb in the HbVs inputted at 3% (i.e., 0.02 g/dL) was released into the culture supernatant. This Hb concentration was calculated as ~3 μM. According to the report by Fowler et al.,[25] 1 μM of recombinant Hb did not affect the proliferation of erythroid or myeloid lineage cells from human bone marrow $CD34^+$ cells in liquid culture system. Therefore, we do not believe that the released Hb accounted for the inhibitory effect of long-term exposure to HbVs on the progenitor activity.

It is difficult to predict the events *in vivo* from the results of experiments *in vitro*, because the effects of HbVs on the immature hematopoietic stem/progenitor cells from the CB may not be the same as those on the hematopoietic stem/progenitor cells in the adult bone marrow. In addition, the concentration of HbVs used here is based on simple assumption and may not necessarily be relevant to the physiological conditions prevailing in humans. With regard to the exposure time to HbVs, continuous exposure of hematopoietic stem/progenitor cells to HbVs in the marrow for more than 10 days is unlikely in the clinical setting. Rather, 1-3 days exposure is

more relevant to the clinical setting, because a study in which an acute 40% exchange transfusion of HbVs was administered to rats showed that a significant amount of the HbVs was phagocytosed by the macrophages in the marrow by 1-3 days after the infusion. A significant decrease in the number of HbVs was observed at 7 days, with the vesicles becoming undetectable at 14 days. Under these conditions, hematopoietic activity, including the formation of erythroblastic islets was observed at 3 days in the marrow.[14] Moreover, the destination of HbVs in the bone marrow is macrophages, and the HbVs are degraded in the phagosomes. These findings imply that there is little possibility of direct contact between HbVs and the hematopoietic progenitor cells *in vivo*. The finding that short-term exposure to HbVs did not have any significant effect on the clonogenic activity or the proliferation and differentiation of erythroid and myeloid lineage cells in liquid culture is consistent with the results of animal experiments,[14][15] suggesting that the infusion of HbVs in humans may have no adverse effects on hematopoiesis.

In conclusion, our results suggest that HbVs, under conditions relevant to the clinical setting, have no adverse effect on human CB hematopoietic progenitor activity *in vitro*. The present results are of value for estimating the biocompatibility of HbVs and hematopoietic progenitor cells.

Acknowledgements

The authors thank Prof. Koichi Kobayashi and Dr. Hirohisa Horinouchi (School of Medicine, Keio University) for their meaningful discussions.

REFERENCES

1 Djordjevich L,Miller IF. Synthetic erythrocytes from lipid encapsulated hemoglobin. *Exp Hematol* 1980; **8**: 584-592. Links

2 Phillips WT,Klipper RW,Awasthi VD,Rudolph AS,Cliff R,Kwasiborski V,Goins BA. Polyethylene glycol-modified liposome-encapsulated hemoglobin: A long circulating red cell substitute. *J Pharmacol Exp Ther* 1999; **288**: 665-670. Links

3 Chang TM. Hemoglobin-based red blood cell substitutes. *Artif Organs* 2004; **28**: 789-794. Links

4 Sakai H,Takeoka S,Park SI,Kose T,Nishide H,Izumi Y,Yoshizu A,Kobayashi K,Tsuchida E. Surface modification of hemoglobin vesicles with poly(ethylene glycol) and effects on aggregation, viscosity, and blood flow during 90% exchange transfusion in anesthetized rats. *Bioconjugate Chem* 1997; **8**: 23-30. Links

5 Sakai H,Masada Y,Horinouchi H,Yamamoto M,Ikeda E,Takeoka S,Kobayashi K,Tsuchida E. Hemoglobin-vesicles suspended in recombinant human serum albumin for resuscitation from hemorrhagic shock in anesthetized rats. *Crit Care Med* 2004; **32**: 539-545. Links

6 Cabrales P,Sakai H,Tsai AG,Takeoka S,Tsuchida E,Intaglietta M. Oxygen transport by low and normal oxygen affinity hemoglobin vesicles in extreme hemodilution. *Am J Physiol Heart Circ Physiol* 2005; **288**: H1885-H1892. Links

7 Yoshizu A,Izumi Y,Park S,Sakai H,Takeoka S,Horinouchi H,Ikeda E,Tsuchida E,Kobayashi K. Hemorrhagic shock resuscitation with an artificial oxygen carrier, hemoglobin vesicle, maintains intestinal perfusion and suppresses the increase in plasma tumor necrosis factor-α. *ASAIO J* 2004; **50**: 458-463. Links

8 Wakamoto S,Fujihara M,Abe H,Yamaguchi M,Azuma H,Ikeda H,Takeoka S,Tsuchida E. Effects of hemoglobin vesicles on resting and agonist-stimulated human platelets in vitro. *Artif Cells Blood Subs Biotechnol* 2005; **33**: 101-111. Links

9 Ito T,Fujihara M,Abe H,Yamaguchi M,Wakamoto S,Takeoka S,Sakai H,Tsuchida E,Ikeda H,Ikebuchi K. Effects of poly(ethyleneglycol)-modified hemoglobin vesicles on *N*-formyl-methionyl-leucyl-phenylalanine-induced responses of polymorphonuclear neutrophils in vitro. *Artif Cells Blood Substit Immobil Biotechnol* 2001; **29**: 427-437. Links

10 Abe H,Fujihara M,Azuma H,Ikeda H,Ikebuchi K,Takeoka S,Tsuchida E,Harashima H. Interaction of hemoglobin vesicles, a cellular-type artificial oxygen carrier, with human plasma: Effects on coagulation, kallikrein-kinin, and complement systems. *Artif Cells Blood Substit Immobil Biotechnol* 2006; **34**: 1-10. Links

11 Torchilin VP. Recent advances with liposomes as pharmaceutical carriers. *Nat Rev Drug Discov* 2005; **4**: 145-160. Links

12 Sou K,Klipper R,Goins B,Tsuchida E,Phillips WT. Circulation kinetics and organ distribution of Hb-vesicles developed as a red blood cell substitute. *J Pharmacol Exp Ther* 2005; **312**: 702-709. Links

13 Sakai H,Horinouchi H,Tomiyama K,Ikeda E,Takeoka S,Kobayashi K,Tsuchida E. Hemoglobin-vesicles as oxygen carriers: Influence on phagocytic activity and histopathological changes in reticuloendothelial system. *Am J Pathol* 2001; **159**: 1079-1088. Links

14 Sakai H,Horinouchi H,Yamamoto M,Ikeda E,Takeoka S,Takaori M,Tsuchida E,Kobayashi K. Acute 40 percent exchange-transfusion with hemoglobin-vesicles (HbV) suspended in recombinant human serum albumin solution: Degradation of HbV and erythropoiesis in a rat spleen for 2 weeks. *Transfusion* 2006; **46**: 339-347. Links

15 Abe H,Azuma H,Yamaguchi M,Fujihara M,Ikeda H,Sakai H,Takeoka S,Tsuchida E. Effects of hemoglobin vesicles, a liposomal artificial oxygen carrier, on hematological responses, complement and anaphylactic reactions in rats. *Artif Cells Blood Substit Immobil Biotechnol* 2007; **35**: 157-172. Links

16 Pessina A,Malerba I,Gribaldo L. Hematotoxicity testing by cell clonogenic assay in drug development and preclinical trials. *Curr Pharm Des* 2005; **11**: 1055-1065. Links

17 Sakai H,Yuasa M,Onuma H,Takeoka S,Tsuchida E. Synthesis and physicochemical characterization of a series of hemoglobin-based oxygen carriers: Objective comparison between cellular and acellular types. *Bioconjugate Chem* 2000; **11**: 56-64. Links

18 Sou K,Naito Y,Endo T,Takeoka S,Tsuchida E. Effective encapsulation of proteins into size-controlled phospholipid vesicles using freeze-thawing and extrusion. *Biotechnol Prog* 2003; **19**: 1547-1552. Links

19 Sakai H,Hisamoto S,Fukutomi I,Sou K,Takeoka S,Tsuchida E. Detection of lipopolysaccharide in hemoglobin-vesicles by Limulus amebocyte lysate test with kinetic-turbidimetric gel clotting analysis and pretreatment of surfactant. *J Pharm Sci* 2004; **93**: 310-321. Links

20 Lipton JM,Nathan DG. The anatomy and physiology of hematopoiesis. In: Nathan DG ,Oski FA. editors. *Hematology of Infancy and Childhood*. Philadelphia: WB Saunders; 1987. p 128-158.

21 Ohkawara JI,Ikebuchi K,Fujihara M,Sato N,Hirayama F,Yamaguchi M,Mori KJ,Sekiguchi S. Culture system for extensive production of CD19+IgM+ cells by human cord blood CD34+ progenitors. *Leukemia* 1998; **12**: 764-771. Links

22 Giarratana MC,Kobari L,Lapillonne H,Chalmers D,Kiger L,Cynober T,Marden MC,Wajcman H,Douay L. Ex vivo generation of fully mature human red blood cells from hematopoietic stem cells. *Nat Biotechnol* 2005; **23**: 69-74. Links

23 Unverzagt KL,Bender JG,Loudovaris M,Martinson JA,Hazelton B,Weaver C. Characterization of a culture-derived CD15+CD11b- promyelocytic population from CD34+ peripheral blood cells. *J Leukoc Biol* 1997; **62**: 480-484. Links

24 Teramura Y,Kanazawa H,Sakai H,Takeoka S,Tsuchida E. Prolonged oxygen-carrying ability of hemoglobin vesicles by coencapsulation of catalase in vivo. *Bioconjugate Chem* 2003; **14**: 1171-1176. Links

25 Fowler DA,Rsosenthal GJ,Sommadossi JP. Effect of recombinant human hemoglobin on human bone marrow progenitor cells: protection and reversal of 3′-azido-3′-deoxythymidine-induced toxicity. *Toxicol Lett* 1996; **85**: 55-62. Links

Wiley InterScience :: Article :: HTML Full Text 08/03/14 20:34

Available online at www.sciencedirect.com
ScienceDirect
Biomaterials 28 (2007) 2655–2666
Biomaterials
www.elsevier.com/locate/biomaterials

Selective uptake of surface-modified phospholipid vesicles by bone marrow macrophages *in vivo*

Keitaro Sou[a], Beth Goins[b], Shinji Takeoka[a], Eishun Tsuchida[a,*], William T. Phillips[b]

[a]*Advanced Research Institute for Science and Engineering, Waseda University, Tokyo 169-8555, Japan*
[b]*Department of Radiology, University of Texas Health Science Center at San Antonio, 7703 Floyd Curl Drive, San Antonio, TX 78229-3900, USA*

Received 29 August 2006; accepted 31 January 2007
Available online 20 February 2007

Abstract

An advantage of using vesicles (liposomes) as drug delivery carriers is that their pharmacokinetics can be controlled by surface characteristics, which can permit specific delivery of the encapsulated agents to organs or cells *in vivo*. Here we report a vesicle formulation which targets the bone marrow after intravenous injection in rabbits. Surface modification of the vesicle with an anionic amphiphile; L-glutamic acid, *N*-(3-carboxy-1-oxopropyl)-, 1,5-dihexadecyl ester (SA) results in significant targeting of vesicles to bone marrow. Further incorporation of as little as 0.6 mol% of poly(ethylene glycol)-lipid (PEG-DSPE) passively enhanced the distribution of SA-vesicles into bone marrow and inhibited hepatic uptake. In this model, more than 60% of the intravenously injected vesicles were distributed to bone marrow within 6 h after administration of a small dose of lipid (15 mg/kg b.w.). Histological evidence indicates that the targeting was achieved due to uptake by bone marrow macrophages (BMMϕ). The efficient delivery of encapsulated scintigraphic and fluorescent imaging agents to BMMϕ suggests that vesicles are promising carriers for the specific targeting of BMMϕ and may be useful for delivering a wide range of therapeutic agents to bone marrow.

Keywords: Nanoparticle; Liposome; Bone marrow; Macrophage; Drug delivery; Surface modification

1. Introduction

Nanoparticulate carrier systems have been investigated as candidates for targeted delivery in cancer therapy and gene therapy [1,2]. A wide variety of nanoparticle systems have been developed for biological applications. One of the advantages of using nanoparticulate materials is based on their controllable surface properties which permit specific interactions with cells, tissues, and organs. Although a number of investigators have demonstrated that endocytosis of nanoparticles *in vitro* is accelerated by surface modification of the particles with specific ligands, the specific *in vivo* targeting of cells remains challenging because it is hindered by competing interactions, especially fairly high mononuclear phagocyte system (MPS) uptake *in vivo*.

Phospholipid vesicles (liposomes) have been widely investigated as potential carriers for drugs, genes, and proteins because their capsular structure permits encapsulation of various therapeutic agents [2–4]. Because of their particulate nature, these vesicles are trapped in the MPS, particularly hepatic Kupffer cells and spleen macrophages following intravenous administration [5,6]. Once in the bloodstream, the binding of plasma proteins such as immunoglobulins, complement proteins, apolipoproteins, etc., which together are termed "opsonins" on the vesicular surface have been reported to accelerate phagocytosis of the vesicles by macrophages, because the macrophages have scavenger receptors to bind the opsonins [5]. In addition to this mechanism, vesicles containing anionic phospholipids such as phosphatidylserine (PS), which are markers of apoptotic cells, have been reported to bind with a PS receptor on macrophages [7]. Improved vesicles with

*Corresponding author. Tel.: +81 3 5286 3120; fax: +81 3 3205 4740.
E-mail addresses: ksou@waseda.jp (K. Sou), eishun@waseda.jp (E. Tsuchida).

0142-9612/$ - see front matter © 2007 Elsevier Ltd. All rights reserved.
doi:10.1016/j.biomaterials.2007.01.041

prolonged circulation times preventing MPS uptake have been formulated with poly(ethylene glycol) (PEG) derivatives [8]. These vesicles have been termed as stealth liposomes, due to their ability to evade uptake by the macrophage, particularly Kupffer cells. Long circulating liposomes with PEG surface modification are currently being used as anti-cancer drug delivery agents [9].

On the other hand, the phagocytic ability of the MPS contributes to achieving an active targeting of particulate carriers to macrophages [10,11]. Macrophages produce a wide range of biologically active molecules that are both beneficial and detrimental. Many of the detrimental effects of macrophages are associated with their pro-inflammatory effects. Thus, interventions targeted to macrophages may open new therapeutic approaches for controlling diseases associated with inflammation. Evidence from a number of sources suggests that cancer-associated inflammation promotes tumor growth and progression, and tumor-associated macrophages play a critical role in the initiation, maintenance, and resolution of inflammation [12]. These tumor-associated macrophages are inactivated by mediators from tumor cells, and they serve to promote tumor growth. The importance of macrophages in disease development has led a number of researchers to investigate methods for the site-specific delivery of drugs to macrophages.

Bone marrow, which contains macrophages, is one of the organs responsible for uptake of circulating particulate materials [5,9,13–17]. Also, macrophages associated with erythroblasts in a hematopoietic environment participate in erythropoiesis control, and engulfment of nuclei from erythroid precursor cells [18,19]. The development of drug delivery systems with specific bone marrow targeting may have therapeutic benefits for hematological malignancies as well as hemopoiesis control. However, very little attention has been paid to bone marrow as part of the MPS because its contribution to the overall MPS is generally much less than that of the liver and spleen *in vivo*. Another essential problem for targeting of BMMϕ is caused by lack of understanding of their specific targeting receptor. Therefore, development of a method for specifically targeting bone marrow will be facilitated by knowledge of the strategies to allow nanoparticles to escape from liver and spleen uptake, but not from bone marrow uptake, and development of specific ligands to induce targeting of bone marrow MPS.

Recently, we have discovered a vesicular formulation which shows remarkable targeting to rabbit bone marrow even when administered at small lipid doses. In this article, we address the components of this vesicle responsible for the targeting of bone marrow and additional vesicular modifications for escaping from liver and spleen uptake, but not from bone marrow. These results may be widely applied to the design of nanoparticulate carriers that target the bone marrow. Bone marrow targeting carriers could open up a wide variety of new therapeutic applications.

2. Materials and methods

2.1. Materials

1,2-Dipalmitoyl-*sn*-glycero-3-phosphocholine (DPPC) and cholesterol (CH) were purchased from Nippon Fine Chemical Co. Ltd. (Osaka, Japan); 1,2-distearoyl-*sn*-glycero-3-phosphoethanolamine-*N*-[monomethoxy poly(ethylene glycol) (5000)] (PEG-DSPE) was purchased from NOF Co. (Tokyo, Japan). L-glutamic acid, *N*-(3-carboxy-1-oxopropyl)-, 1,5-dihexadecyl ester (SA) was synthesized as previously reported [20]. Glutathione was purchased from Sigma (St. Louis, MO). Superoxide dismutase (SOD) was purchased from Wako Pure Chemical Industries Ltd. (Osaka, Japan). 4,4-difluoro-5-methyl-4-bora-3a,4a-diaza-s-indacene-3-dodecanoic acid (C_1-BODIPY C_{12}) and Texas Red (TR) sulfonyl chloride were purchased from Molecular Probes, Inc. (Eugene, OR).

2.2. Preparation of vesicles

All vesicle preparations were performed under sterile conditions. DPPC and CH (1:1 molar ratio), or DPPC, CH, and SA (1:1:0.2 molar ratio) were dissolved in benzene and lyophilized to lipid powders. The mixed lipid powder was hydrated with a glutathione (30 mM) and NaCl (120 mM) solution (pH: 7.0) at 5 g dL^{-1}, and submitted to three cycles of freeze–thawing. After controlling vesicle size by an extrusion method (final pore size of the filter: 0.22 μm, Fuji microfilter, Fuji Photo Film Co., Tokyo, Japan), the unencapsulated glutathione was removed by three ultracentrifugation steps ($3 \times 10^5 g$, 60 min each) and the vesicles were dispersed in saline solution. Surface modification with PEG was performed by making use of the spontaneous incorporation of PEG-DPSE into vesicles [21]. Various concentrations of the PEG-DSPE dispersion were added to the vesicle dispersion and the mixture incubated at 37 °C for 3 h. The vesicle dispersion was ultracentrifuged ($3 \times 10^5 g$, 60 min) to remove unincorporated PEG-DSPE in the supernatant. After washing the precipitated vesicle pellet by ultracentrifugation ($3 \times 10^5 g$, 60 min), the PEG-modified vesicles (PEG-vesicles) were dispersed in saline at 7 g dL^{-1}, and the dispersion was then passed through a sterilized membrane filter (pore size 0.45 μm, DISMIC filter 45, ADVANTEC). The amount of PEG-DSPE incorporated was determined from the peak area ratio of methylene protons of PEG-DSPE (3.63 ppm) to the choline methyl protons of DPPC (3.39 ppm) using ^{1}H-NMR spectroscopy (JEOL JNM-LA500) [21]. SA-vesicles containing 0.3, 0.6, 1.4, and 2.6 mol% of PEG-DSPE on the surface (represented as PEG(0.3)-, PEG(0.6)-, PEG(1.4)-, and PEG(2.6)-[SA-Ve], respectively) and control vesicles containing 2.6 mol% of PEG-DSPE (represented as PEG(2.6)-Ve) were prepared and characterized for these studies. The diameter of the resulting vesicles was determined with a COULTER submicron particle analyzer (N4SD, Coulter, Hialeah, FL), and represented as an average diameter ± standard deviation (SD). Endotoxin contamination was determined to be below 0.1 EU/mL by the Limulus assay test [22].

2.3. Technetium-99m (^{99m}Tc)-labeling of vesicles

Radiolabeling of vesicles was performed according to a method described previously [14,17,23,24]. A saline solution of sodium [^{99m}Tc]pertechnetate (5 mL, 2.78 GBq (75 mCi)) (GE Healthcare Radiopharmacy, San Antonio, TX) was injected into a vial containing lyophilized hexamethylpropyleneamine oxime (HMPAO; 0.5 mg, $SnCl_2$; 7.6 μg) (Ceretec™; GE Healthcare, Arlington, IL). The mixed solution was incubated for 5 min at room temperature. The ^{99m}Tc-HMPAO solution (1 mL) was then added to the vesicle dispersion ([lipids] = 7 g dL^{-1}, 1 mL), and the resulting mixture was incubated for 1 h. After removing free ^{99m}Tc-HMPAO by gel filtration (Sephadex-G25 column), total radioactivity was measured in a dose calibrator (Radex, Mark 5 Model, Houston, TX) and the labeling efficiency was calculated as the percentage of radioactivity in ^{99m}Tc-vesicles to radioactivity measured just before gel filtration.

2.4. Labeling stability of ^{99m}Tc-labeled vesicles in vitro

Labeling stability was examined *in vitro* according to a previously reported procedure [25]. Prepared ^{99m}Tc-labeled vesicle dispersions (0.5 mL) were mixed with rabbit serum (1.5 mL) and incubated at 37 °C to check the labeling stability. A 100 μL aliquot of incubated sample at 24 and 48 h after mixing was passed through a Bio Gel A-15 m (200–400 mesh) spin column. The sample was eluted by sequential addition of 100 μL of Dulbecco's phosphate-buffered saline (pH 7.3) under the centrifugal force of 1000 rpm for 1 min. Each fraction was collected separately and counted in a scintillation well counter (Canberra multichannel analyzer; Canberra Industries, Meriden, CT). Another 100 μL aliquot of incubation sample was used as a standard. The sum total of activity eluted with vesicle fractions was compared with total radioactivity in the standard. As for ^{99m}Tc-labeled PEG(0.6)-[SA-Ve], the labeling stability was also examined in human plasma at 37 °C for 24 h.

2.5. Animal experiments

Animal experiments were performed under the National Institutes of Health Animal Use and Care guidelines and approved by the University of Texas Health Science Center at San Antonio Institutional Animal Care Committee. Male New Zealand White rabbits (2–3 kg, $n = 3$–4 per each vesicle formulation) were anesthetized with an intramuscular injection of ketamine/xylazine (both from Phoenix Scientific, St. Joseph, MO) mixture (50 and 10 mg/kg body weight (b.w.), respectively). One ear of a rabbit was catheterized with a venous line, and the other ear was catheterized with an arterial line. ^{99m}Tc-vesicles were infused into the venous line at 1 mL/min and blood samples were drawn from the arterial line. Each rabbit received a total dose of 214.6–377.4 MBq (5.8–10.2 mCi) ^{99m}Tc-activity and 15 mg/kg b.w. of lipids. As a control study, ^{99m}Tc-HMPAO solution (3 mL) was mixed with glutathione solution (30 mM, 3 mL), and the mixed solution was infused into the venous line at 1 mL/min in rabbits. Each rabbit received a total dose of 321.9–399.6 MBq (8.7–10.8 mCi) ^{99m}Tc-activity.

2.6. Imaging study

Rabbits were placed in the supine position under a Picker (Cleveland, OH) large-field-of-view gamma camera using a low-energy all-purpose collimator and interfaced with a Pinnacle imaging computer (Medasys, Ann Arbor, MI). One-minute dynamic 64 × 64 pixel scintigraphic images were acquired over a continuous period of 1.5 h after the injection of ^{99m}Tc-vesicles. Static images were also acquired at various times post-injection. The image analysis was performed using a nuclear medicine analysis workstation (Pinnacle computer; Medasys, Ann Arbor, MI). The regions of interest were drawn around images of the whole body, one femur, liver, and spleen. The radioactivity counts were decay-corrected at each time, and converted to a percentage of whole body counts. Corrections were made for the blood pool contribution of each organ using the percent injected dose (%ID) measured immediately after infusion.

2.7. Blood persistence and biodistribution

Blood was collected from the arterial line of the rabbit (100 μL) at various times post-injection. The radioactivity of blood samples was quantified in a scintillation well counter (Canberra Multichannel Analyzer, Meridan, CT) during the same counting session. The counts at each time were converted to the percentage of the counts in the sample collected immediately after injection. The animals were rapidly sacrificed at 6 or 24 h and the tissue samples were collected, weighed and counted for radioactivity in the same scintillation well counter for calculation of biodistribution. To calculate the %ID per organ, total blood volume, muscle and skin mass were estimated as 5.7%, 45%, and 10% of total body weight, respectively [26,27]. Bone mass was estimated to be 12 times that of one femur [28].

2.8. Microscopic study

Histological examination of fluorescence delivered into bone marrow tissues was performed using PEG(0.6)-[SA-Ve], double fluorescently labeled by encapsulating SOD conjugated by TR sulfonyl chloride (TR-SOD) in inner aqueous phase and embedding C_1-BODIPY C_{12} in bilayer membrane. Conjugation of TR-SOD to SOD was performed according to previously reported procedure [29], and purified TR-SOD was encapsulated in mixed lipids including 1 mol% of C_1-BODIPY C_{12} to obtain the double fluorescently-labeled PEG(0.6)-[SA-Ve] with size of 247 ± 22 nm in diameter. Labeled vesicles were i.v. injected into anesthetized Male New Zealand White rabbits (2.5 kg, lipids: 15 mg/kg b.w.). At 6 h after injection, femoral bone marrow tissues, liver and spleen were taken, fixed in 10% formalin solution, and then sliced into sections. The sections were fixed on the glass slides with agar at 4 °C and examined with a confocal scanning microscope (Olympus IX-70). Transmission electron microscopic (TEM) observation was performed to observe the bone marrow tissues at a higher magnification. PEG(0.6)-[SA-Ve] were i.v. injected into anesthetized Male New Zealand White rabbits (2.5 kg). The rabbits received 15 mg/kg b.w. of lipids. Control rabbits received no injection. Bone marrow was taken from the left femur of rabbits at 6 h after injection of vesicles, and fixed in 2.5% glutaraldehyde solution. The fixed bone marrow was then washed with 0.1 mol/L phosphate buffer, pH 7.4, and stained with 2% osmic acid solution at 4 °C for 2 h. The organs were first dehydrated stepwise with ethanol, and then polymerized using Quetol 812 at 60 °C for 28 h. The obtained samples were sliced into sections by using an Ultracut S microtome. The sliced samples were stained with 3% uranyl acetate solution for 20 min and then treated with Satoh's lead solution (lead acetate, lead nitrate, and lead citrate) in citrate for 5 min, washed, and dried. The sample was observed and a picture taken with a transmission electron microscope (TEM, H-7500, Hitachi, Tokyo, Japan).

2.9. Theoretical estimation

The theoretical estimation for surface coverage by PEG on vesicles has been reported previously [30,31]. At low grafting densities of PEG, the chains of grafted-PEG are displayed "mushrooms", in which area A_{PEG} covered by each molecule is theoretically calculated as

$$A_{PEG} = \pi R_F^2, \quad (1)$$

where the Flory radius R_F is given by

$$R_F = N^{3/5} a, \quad (2)$$

where N is the degree of polymerization, a is the size of a monomer.

The percentage of covered surface area by PEG in the mushroom conformation R was estimated as

$$R = A_{PEG} \times M / A_{lipid}, \quad (3)$$

where M is the mole percentage of PEG-DSPE and A_{lipid} is the average area of total membrane lipids. In subsequent calculation, we used $N = 114$ and $a = 0.35$ nm for PEG (Mw 5000), and $A_{lipid} \approx 0.4\,nm^2$ for average area as mixed membrane of DPPC and CH (1:1 molar ratio) [32].

2.10. Statistical methods

Values are reported as mean ± standard error of the mean (SEM). Statistical analysis was performed using Microsoft Excel for Windows. Biodistribution data were compared using the Student's unpaired t-test. A p-value <0.01 or 0.05 was considered statistically significant.

3. Results

3.1. Surface modification and radiolabeling

The average diameter of vesicles was controlled to 270 nm by the stepwise extrusion through cellulose acetate membrane filters with a final pore size of 0.22 μm as shown in Table 1. The surface of the vesicles were modified during spontaneous incorporation of PEG conjugated to 1,2-distearoyl-*sn*-glycero-3-phosphoethanolamine (DSPE) into the lipid bilayer of preformed vesicles. The incorporation efficiency of PEG-DSPE was approximately 85%, independent of the added amount. Theoretically, the surface of PEG (0.3)-[SA-Ve] is not fully covered with PEG chains in mushroom conformation (theoretically calculated covered surface area: 85%), and surface coverage is completed with >0.6 mol% of PEG-DSPE. The ^{99m}Tc-labeling efficiency was approximately 84%, independent of the vesicular formulation. Since the ^{99m}Tc was located in the inner aqueous phase of vesicles encapsulating glutathione, the surface properties would not have been altered by the labeling procedure. The incubation of labeled ^{99m}Tc-vesicles in rabbit serum for 48 h revealed that more than 95% of the incorporated ^{99m}Tc remained in the prepared vesicles, regardless of the composition of the vesicles. Also in human plasma, 98% of incorporated ^{99m}Tc remained with PEG(0.6)-[SA-Ve] at 24 h. These data indicate that the labeling procedure results in a stably labeled vesicle preparation and maintains the ^{99m}Tc within vesicles, even during incubation in plasma at 37 °C.

3.2. Circulation kinetics and biodistribution

First, the circulation kinetics and organ distribution of several formulations were compared to determine the optimized component for targeting bone marrow. For this purpose, scintigraphy was superior to other methods because it was possible to quantitatively determine the organ distribution of the injected vesicles in whole body. The elimination rate of SA-Ve from circulating blood was much faster compared with that of control vesicles (Ve): the circulating half-life times ($t_{1/2}$s) of the SA-Ve and Ve were 0.6 and 9.4 h at injection dose of 15 mg/kg b.w. (Fig. 1(A)). Incorporation of as little as 0.3 mol% of PEG-DSPE did not affect the circulation time of SA-Ve. Incorporation of above 0.6 mol% of PEG-DSPE prolonged the circulation time of SA-Ve and the $t_{1/2}$ increased with increasing amounts of PEG-DSPE incorporation as summarized in Table 1. The incorporation of 2.6 mol% of PEG-DSPE also gave a remarkable improvement in circulation time for control Ve ($t_{1/2}$: 24.8 h). At 24 h post injection, the radioactivity of excised organs was counted using a scintillation counter. Major organs exhibiting the uptake of vesicles were bone marrow and liver for SA-Ve (Figs. 1(B) and (C)), while liver and spleen were the organs with the highest accumulation of control Ve (Figs. 1(C) and (D)). PEG modification clearly inhibited hepatic uptake of both SA-Ve and control Ve, and this effect became significant as the amount of PEG-DSPE incorporated increased (Fig. 1(C)). While a maximum amount of SA-Ve was observed in bone marrow when the SA-Ve contained 0.6 mol% PEG-DSPE, further incorporation of PEG-DSPE led to a decrease in the distribution of SA-Ve in bone marrow (Fig. 1(B)). Other organs apart from kidney and muscle for PEG(2.6)-[SA-Ve] exhibited only a small amount of activity (<1%ID, Supplementary Table 1 online). Injection in rabbits of a mixed solution of ^{99m}Tc-HMPAO and glutathione in a similar ratio as would be found within ^{99m}Tc-vesicles served as a control study of the radiolabeling agents without encapsulation within the vesicles. As shown in Fig. 2(A), injection of ^{99m}Tc-HMPAO/glutathione was rapidly eliminated from blood circulation ($t_{1/2}$: 3 min), and gamma camera images indicated that the labeling agents were rapidly excreted in urine through the kidney (Fig. 2(B)). Region of interest analysis showed that 67.1±0.8% of injected radioactivity was detected in bladder within 1 h after injection (Fig. 2(C)). At 6 h, biodistribution data also showed significant radioactivity in the urine (76.91±4.80%ID) and kidney (6.11±0.53%ID), but other organs including bone marrow had only minimal %ID dose uptake as summarized in Table 2. This control study shows that a mixture of ^{99m}Tc-HMPAO and glutathione is rapidly removed from the blood by renal excretion, which is

Table 1
Specification of prepared vesicles

Sample[a]	Mean diameter±SD (nm)	PEG-DSPE (mol%)	$t_{1/2}$ (h)[b]
SA-Ve	269±11	0	0.6
PEG(0.3)-[SA-Ve]	276±13	0.3	0.6
PEG(0.6)-[SA-Ve]	273±12	0.6	1.0
PEG(1.4)-[SA-Ve]	275±12	1.4	3.9
PEG(2.6)-[SA-Ve]	274±12	2.6	5.4
Ve	262±43	0	9.4
PEG(2.6)-Ve	259±74	2.6	24.8

[a]SA-Ve is based on DPPC/CH/SA (molar ratio, 1:1:0.2), and Ve is DPPC/CH (molar ratio, 1:1) as a control sample. PEG-modified samples were prepared using the spontaneous incorporation of PEG-DSPE into the prepared SA-Ve or Ve.
[b]The $t_{1/2}$ values were calculated from Fig. 1(A) data.

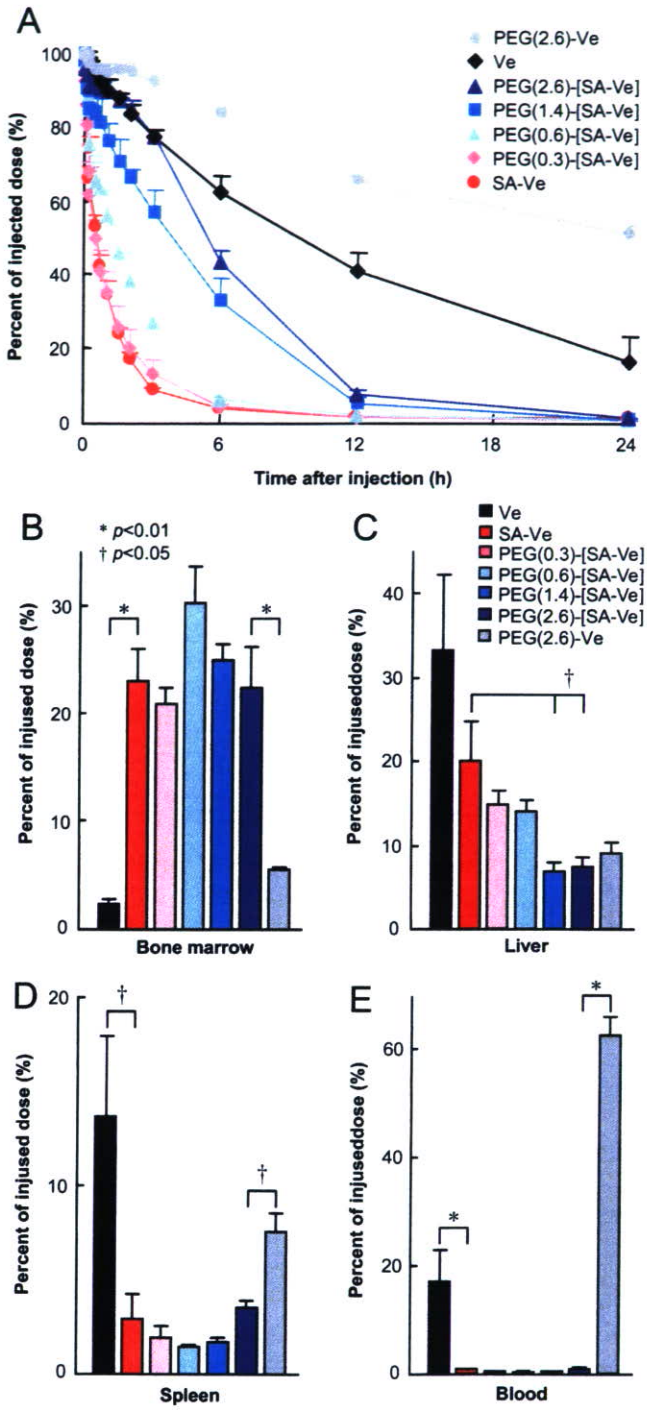

Fig. 1. Effect of surface modification with SA and PEG-DSPE on circulation kinetics and organ distribution of phospholipid vesicles. (A) Circulation kinetics of SA-vesicles (SA-Ve) and control vesicles (Ve) containing various amounts of PEG-DSPE after i.v. infusion (lipids: 15 mg/kg b.w.) in rabbits. ^{99m}Tc radioactivity was quantitated by scintillation counting of blood samples with time. The percentage of injected dose was calculated as a percentage of baseline radioactivity in a blood sample withdrawn just after injection. (B)–(E) Distribution of SA-vesicles (SA-Ve) and control vesicles (Ve) containing various amounts of PEG-DSPE as a percentage of the injected dose in bone marrow (B), liver (C), spleen (D), and blood (E) at 24 h after i.v. infusion in rabbits. *, Statistical significance ($p<0.01$), †, statistical significance ($p<0.05$).

typical of small molecules. These results indicate that the SA-Ve were clearly directed to bone marrow, and the process of accumulation of SA-Ve into bone marrow is correlated with competitive trapping by liver. Surface modification of SA-Ve with the proper amount of PEG-lipids inhibits the trapping of SA-Ve in liver and directs SA-Ve to bone marrow, a process which could be regarded as a combination of active and passive targeting. Conventional anionic vesicles containing phosphatidyl glycerol (PG) were inactive for targeting of bone marrow (Supplementary Table 2 online). The injected PEG(0.6)-[SA-Ve], which was the formulation showing the highest persistence in bone marrow at 24 h, were almost removed from circulation within 6 h (as little as 6.4±0.5%ID of PEG(0.6)-[SA-Ve] was circulating in blood at 6 h). Therefore, the initial distribution kinetics of PEG(0.6)-[SA-Ve] was studied in detail.

3.3. Distribution kinetics of PEG(0.6)-[SA-Ve]

Scintigraphic images clearly showed the injected radioactivity of PEG(0.6)-[SA-Ve] to be redirected from heart and liver, both organs having large blood pool contributions, and increasingly deposited in the bone marrow over time (Fig. 3(A)). The distribution kinetics in bone marrow, liver, and spleen, analyzed from the scintigraphic images, quantitatively indicated that significantly higher doses had accumulated in bone marrow, reaching 68.5±3.3%ID by 6 h after injection (Fig. 3(B)). The biodistribution data calculated from the radioactivity of excised organs also showed that 69.74±0.3%ID of PEG(0.6)-[SA-Ve] had accumulated in bone marrow, as shown in Table 2. At the same time point, liver and spleen had much smaller amounts of 11.51±2.88 and 5.00±1.19%ID, respectively. When ^{99m}Tc-HMPAO/glutathione was injected without encapsulation into PEG(0.6)-[SA-Ve], bone marrow, liver, and spleen had only 1.13±0.24, 1.52±0.14, and 0.01±0.00%ID, respectively. The isolated femur was further separated into soft bone marrow, joint bone (sponge bone), and skeleton and each separate tissue counted for radioactivity. As shown in Fig. 3(C), 66.5±1.1% of radioactivity in one femur was detected in soft bone marrow. The joint bone including soft bone marrow had 28.8±1.3% of radioactivity, and less radioactivity was detected in the separated skeleton (4.7±0.3%). These results indicate that the intravenously injected PEG(0.6)-[SA-Ve] mostly accumulates into soft bone marrow. The gamma camera images clearly show that the bone marrow uptake was evenly distributed over whole bone (Fig. 4), and the localization of radioactivity representing the distribution of PEG(0.6)-[SA-Ve] in these images was analyzed for separate regions. The spine and pelvis had 21.23±0.42% and 18.09±0.60%, values which were much higher than other regions. The right and left femurs had equal radioactivity of 7.97±0.05% and 8.34±0.18%; these values are in agreement with a report

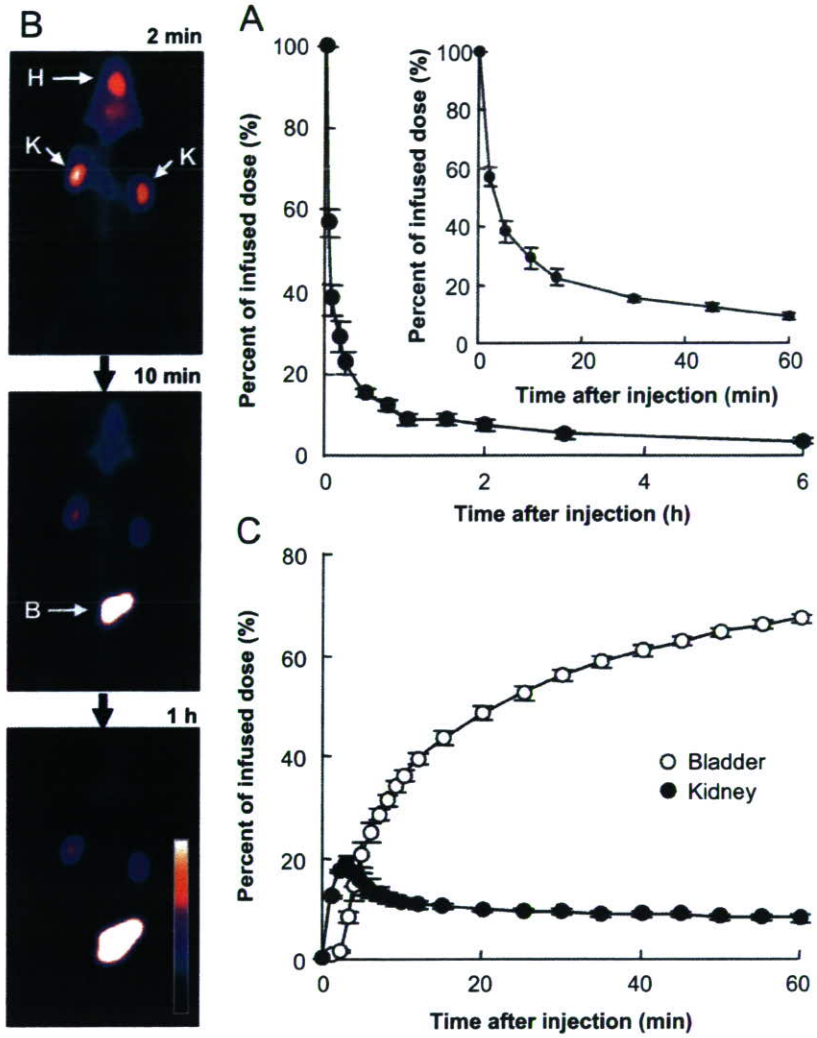

Fig. 2. Circulation and distribution kinetics of mixture of ^{99m}Tc-HMPAO and glutathione without encapsulation in vesicles after i.v. infusion in rabbits. (A) Circulation kinetics (B) Gamma camera images of rabbits acquired at various times after infusion. H: heart, K: kidney, B: bladder. (C) Distribution profiles as a percentage of the injected dose analyzed from the gamma camera images.

describing the relationship of 12 times that of a femur as being equivalent to whole bone in rabbits [28].

3.4. Microscopic localization of PEG(0.6)-[SA-Ve] in bone marrow

The initial studies were designed to demonstrate that PEG(0.6)-[SA-Ve] functions as a nanoparticulate carrier as well as identify their microscopic localization in tissues. We used PEG(0.6)-[SA-Ve] double-labeled by encapsulating water-soluble TR-SOD in an aqueous phase and embedding lipid-soluble C_1-BODIPY C_{12} in bilayer membrane (Fig. 5(A)). As shown in Fig. 5(B), the bone marrow sections have fluorescence from both the TR-SOD and C_1-BODIPY C_{12}. The fluorescence was locally concentrated, and larger fluorescent domain was 30 μm in size along the long axis. Fluorescent distribution in red pulp of spleen was dense, whereas it was sparse in liver. An important finding from this observation is that the fluorescence from membrane probes and encapsulated probes are co-localized in bone marrow. These images clearly indicate that PEG(0.6)-[SA-Ve] functions as a nanoparticle-carrier to deliver the encapsulated agents to bone marrow tissues. A second study was performed to identify the histological location of PEG(0.6)-[SA-Ve] in bone marrow. Femoral bone marrow tissue was taken from rabbit at 6 h after i.v. injection of PEG(0.6)-[SA-Ve] and examined using TEM. TEM observation clearly demonstrated the location of PEG(0.6)-[SA-Ve] in bone marrow (Figs. 6(A) and (B)). A massive number of vesicles were trapped in endosomes and lysosomes of BMMϕ, but no vesicles were observed in cytoplasm and cell nucleus (Fig. 6(B)). The diameter of these vesicles averaged 270 nm which was the original diameter of the intravenously administered PEG(0.6)-[SA-Ve]. Several similar BMMϕ with vesicles in endosomes and lysosomes were observed, while no vesicles were observed

Table 2
Biodistribution of PEG(0.6)-[SA-Ve] and ^{99m}Tc-HMPAO/glutathione as a percent of the injected dose (%ID) and %ID per gram of tissue at 6 h after i.v. infusion in rabbits

Organs	PEG(0.6)-[SA-Ve]		^{99m}Tc-HMPAO/glutathione	
	%ID ± SEM (%)	%ID/g tissue ± SEM (%/g)	%ID ± SEM (%)	%ID/g tissue ± SEM (%/g)
Blood	6.58 ± 2.91	0.065 ± 0.028	3.34 ± 1.68	0.025 ± 0.013
Bone marrow	69.74 ± 0.86	0.806 ± 0.048	1.13 ± 0.24	0.010 ± 0.001
Liver	11.51 ± 2.88	0.237 ± 0.067	1.52 ± 0.14	0.022 ± 0.001
Spleen	5.00 ± 1.19	5.387 ± 0.807	0.01 ± 0.00	0.011 ± 0.001
Bowel	5.85 ± 0.31	0.014 ± 0.000	4.41 ± 0.19	0.009 ± 0.000
Skin	1.57 ± 0.21	0.009 ± 0.001	2.34 ± 0.30	0.010 ± 0.001
Kidney	2.40 ± 0.10	0.148 ± 0.011	6.11 ± 0.53	0.440 ± 0.066
Muscle	1.86 ± 0.17	0.003 ± 0.000	2.60 ± 0.63	0.002 ± 0.001
Lung	0.19 ± 0.03	0.024 ± 0.006	0.12 ± 0.03	0.010 ± 0.001
Heart	0.03 ± 0.01	0.010 ± 0.002	0.03 ± 0.01	0.006 ± 0.001
Brain	0.01 ± 0.00	0.002 ± 0.000	0.01 ± 0.00	0.001 ± 0.000
Testis	0.03 ± 0.01	0.024 ± 0.005	0.02 ± 0.00	0.008 ± 0.002
Urine	3.57 ± 1.74	—	76.91 ± 4.80	—

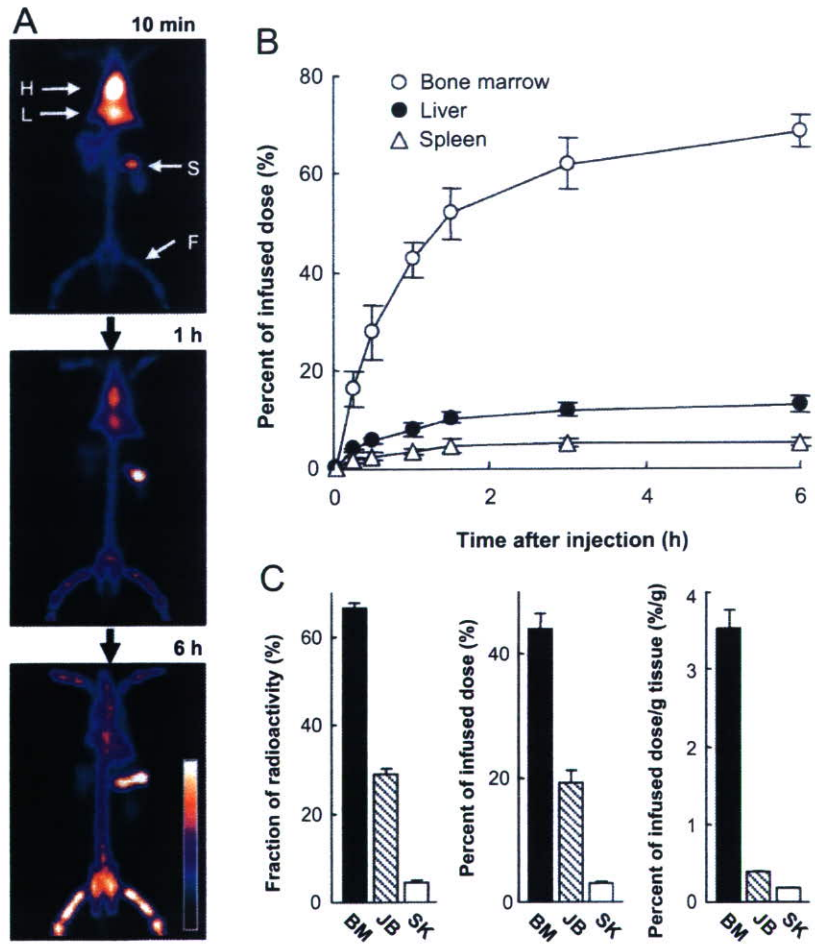

Fig. 3. Initial distribution kinetics of PEG(0.6)-[SA-Ve] after i.v. infusion (lipids: 15 mg/kg b.w.) in rabbits. (A) Gamma camera images of rabbits acquired at various times after infusion. H: heart, L: liver, S: spleen, F: femur. (B) Distribution profiles as a percentage of the injected dose analyzed from the gamma camera images. The total bone marrow was estimated to be 12 times that of one femur. (C) Distribution of radioactivity of PEG(0.6)-[SA-Ve] in separated soft bone marrow (BM), joint bone (sponge bone) (JB), and skeleton (SK) of one femur collected at 6 h after i.v. infusion. Three panels show the fraction of radioactivity, percent of injected dose (%ID), and %ID/g tissue, respectively.

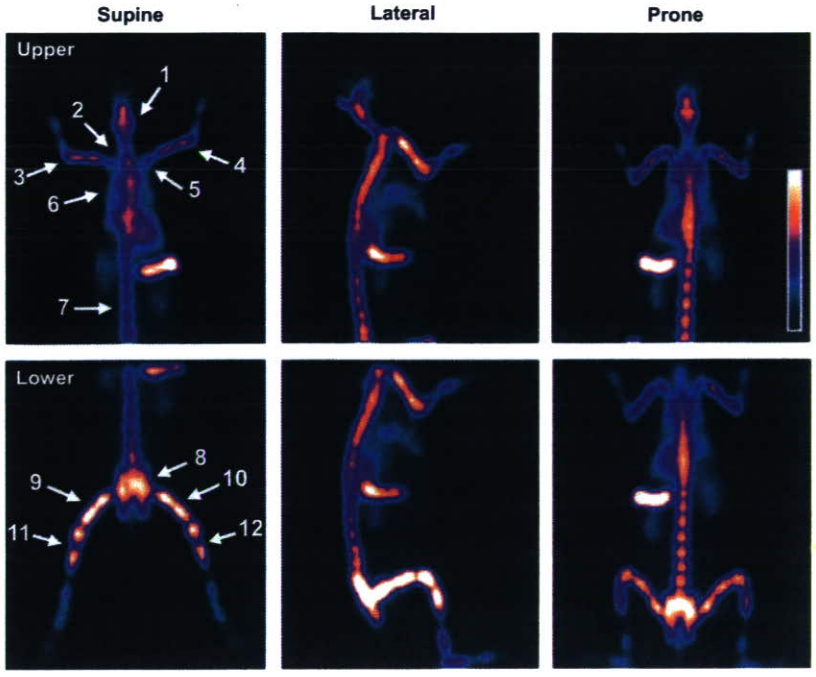

Fig. 4. Gamma camera images of rabbit receiving PEG(0.6)-[SA-Ve], acquired from various angles at 6 h after i.v. infusion. Bone marrow is clearly displayed in these images throughout the rabbit body. Relative radioactivity in separated bone parts were calculated to 1; head (8.41 ± 1.58%), 2; neck (1.10 ± 0.11%), 3; right arm (5.72 ± 0.33%), 4; left arm (5.54 ± 0.40%), 5; shoulder (3.62 ± 0.69%), 6; sternum (4.11 ± 1.35%), 7; spine (21.23 ± 0.42%), 8; pelvis (18.09 ± 0.60%), 9; right femur (7.97 ± 0.05%), 10; left femur (8.34 ± 0.18%), 11; distal right foot (7.88 ± 0.25%), and 12; distal left foot (7.98 ± 0.33%) as percentages to radioactivity of whole bone ± SEM.

in other types of cell such as granular leukocytes, erythroblasts, and endothelial cells in observed section. These microscopic localization studies demonstrate that BMMϕ are the cellular components responsible for clearance of vesicles from the circulation and their uptake by the bone marrow.

4. Discussion

These studies demonstrate that PEG-[SA-Ve] are efficient carriers for targeting the BMMϕ. These vesicles should be useful in the development of bone marrow targeted agents for therapeutic applications. Additionally, this *in vivo* model appears to be an ideal model with which to investigate the role of BMMϕ in the hematopoietic environment. The radiolabeling method for the vesicles encapsulating glutathione with ^{99m}Tc-HMPAO has previously been established for imaging studies [14,23,24]. In the present vesicle formulation, we confirmed the stability of the ^{99m}Tc radiolabeled-vesicles during incubation in serum and plasma at 37 °C for 48 h (more than 95% remaining with vesicles), and we also determined that the free labeling agent is not specifically distributed into organs such as bone marrow, liver, and spleen, but rapidly eliminated through renal excretion as shown in Fig. 2 and Table 2. This evidence provides strong support that the radioisotope distribution reflects the true biodistribution of vesicles. As shown in Fig. 1, comparative data showing the organ distribution of several formulations clearly demonstrated that the uptake of vesicles by bone marrow is induced by the incorporation of SA ($p < 0.01$); furthermore, the incorporation of a small amount of PEG-DSPE on the surface of SA-Ve prolongs its circulation time and tends to enhance the bone marrow selectivity by preventing hepatic uptake. Thus, maximum distribution to bone marrow was observed at 0.6 mol% PEG-DSPE (Fig. 1(B)). The degree of hepatic uptake was reduced as the PEG-DSPE content increased, and this effect became significant above 1.4 mol% ($p < 0.05$). Bone marrow uptake was also reduced above 1.4 mol%. In general, 5–10 mol% of PEG-lipids is incorporated into most of the long circulating vesicle formulations for passive targeting [8,9]. In the present study, prolonged circulation time of vesicles was observed above 0.6 mol% of PEG-DSPE, and the circulation times were prolonged more in vesicles with higher PEG-DSPE content. For the effective targeting of bone marrow, however, higher concentrations of PEG blocked the active targeting of the vesicles to bone marrow. These results indicate that the dense PEG layer on the vesicular surface covers the surface properties having the character of SA and depress uptake by BMMϕ. Therefore, the optimal amount of PEG incorporation was found to be 0.6 mol%, as this concentration passively enhances active targeting. Theoretically, approximately 0.4 mol% of PEG (Mw 5000)-lipids is estimated to be the critical content required to fully cover the vesicle surface which consists of DPPC and CH (1:1 molar ratio) with the mushroom conformation of PEG chains from Eqs. (1) to (3). Thus, it is

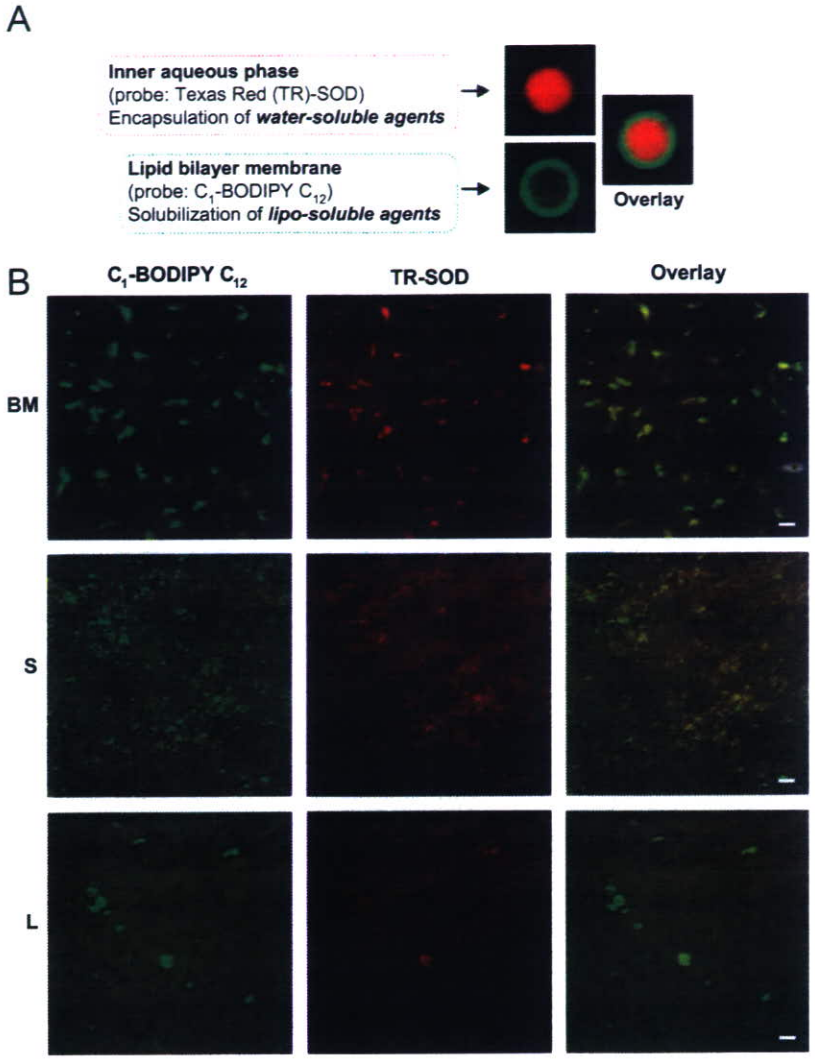

Fig. 5. Histological examination of fluorescence delivered into bone marrow tissues using PEG(0.6)-[SA-Ve] as carriers. (A) Fluorescence localization in double fluorescence-labeled large multilamellar PEG(0.6)-[SA-Ve] with diameter of ca. 10 μm. This observation was performed before extrusion to submicron size to enable observation of the structure within resolution of a confocal microscope. This image indicates that red fluorescence comes from TR-SOD which is encapsulated in inner aqueous phase and green fluorescence comes from C_1-BODIPY C_{12} which is embedded in bilayer membrane. (B) Confocal scanning images of femoral bone marrow (BM), spleen (S), and liver (L) taken from rabbit at 6 h after i.v. injection of double fluorescence-labeled PEG(0.6)-[SA-Ve] with size of 247 ± 22 nm in diameter (lipids: 15 mg/kg b.w.). The scale bars represent 20 μm.

estimated that the optimal incorporation amount of PEG-lipids is slightly higher than that required to fully cover the vesicular surface. This finding provides useful information for the design of vesicle surface to passively enhance the active targeting with PEG-modification *in vivo*.

To examine the participation of the anionic properties of vesicles in BMMϕ uptake, we investigated the organ distribution of conventional anionic vesicles containing PG with same protocol. These PG-vesicles do not distribute to the bone marrow (Supplementary Table 2 online, only 5.36 ± 0.65%ID of PG-vesicles were taken up by the bone marrow at 24 h after i.v. injection). Comparative data for Ve and SA-Ve are shown in Fig. 1(B) and Supplementary Table 1. Previous publications have also supported the observation that PG-vesicles do not distribute to the bone marrow [33], and neutral vesicles with various sizes in the range of 136.2–318 nm do not distribute to the bone marrow [34]. These results indicated that the targeting of bone marrow is not general for neutral vesicles and is achieved not only by the anionic surface of vesicles. The results suggest that SA is specifically responsible for the bone marrow targeting.

Histological observations showed that the vesicles and encapsulated agents are distributed at the same locations into bone marrow tissues, clearly indicating that the encapsulated agents were delivered to the bone marrow tissues by the vesicles (Fig. 5). Higher magnification TEM observations have demonstrated that a massive number of vesicles are trapped in the endosomes and lysosomes of the BMMϕ (Fig. 6). These observations indicated that the